Focus Section: Monitoring During Crisis

Volcano Crisis Management at Piton de la Fournaise (La Réunion) during the COVID-19 Lockdown

Aline Peltier*[1,2], Valérie Ferrazzini[1,2], Andrea Di Muro[1,2], Philippe Kowalski[1,2], Nicolas Villeneuve[1,3], Nicole Richter[1,2,4], Oryaelle Chevrel[5], Jean Luc Froger[5], Alexis Hrysiewicz[5,6], Mathieu Gouhier[5], Diego Coppola[7,8], Lise Retailleau[1,2], François Beauducel[1,9], Lucia Gurioli[5], Patrice Boissier[1,2], Christophe Brunet[1,2], Philippe Catherine[1,2], Fabrice Fontaine[1,2], Frédéric Lauret[1,2], Luciano Garavaglia[1,2], Jacques Lebreton[1,2], Kevin Canjamale[1,2], Nicolas Desfete[1,2], Cyprien Griot[1,2], Andrew Harris[5], Santiago Arellano[10], Marco Liuzzo[11], Sergio Gurrieri[11], and Michael Ramsey[12]

Abstract

In March 2020, the coronavirus disease 2019 outbreak was declared a pandemic by the World Health Organization and became a global health crisis. Authorities worldwide implemented lockdowns to restrict travel and social exchanges in a global effort to counter the pandemic. In France, and in French overseas departments, the lockdown was effective from 17 March to 11 May 2020. It was in this context that the 2–6 April 2020 eruption of Piton de la Fournaise (La Réunion Island, Indian Ocean) took place. Upon the announcement of the lockdown in France, a reduced activity plan was set up by the Institut de Physique du Globe de Paris, which manages the Observatoire Volcanologique du Piton de la Fournaise (OVPF). The aim was to (1) maintain remote monitoring operations by teleworking and (2) authorize fieldwork only for critical reasons, such as serious breakdowns of stations or transmission relays. This eruption provided an opportunity for the observatory to validate its capacity to manage a volcanic crisis with 100% remotely operated monitoring networks. We thus present the long- and short-term precursors to the eruption, and the evolution of the eruption recorded using the real-time monitoring data as communicated to the stakeholders. The data were from both continuously recording and transmitting field instruments as well as satellites. The volcano observatory staff remotely managed the volcano crisis with the various stakeholders based only on these remotely functioning networks. Monitoring duties were also assured in the absence of ad hoc field investigation of the eruption by observatory staff or face-to-face communications. The density and reliability of the OVPF networks, combined with satellite observations, allowed for trustworthy instrument-based monitoring of the eruption and continuity of the OVPF duties in issuing regular updates of volcanic activity in the context of a double crisis: volcanic and health.

Cite this article as Peltier, A., V. Ferrazzini, A. Di Muro, P. Kowalski, N. Villeneuve, N. Richter, O. Chevrel, J. L. Froger, A. Hrysiewicz, M. Gouhier, *et al.* (2020). Volcano Crisis Management at Piton de la Fournaise (La Réunion) during the COVID-19 Lockdown, *Seismol. Res. Lett.* **XX**, 1–15, doi: 10.1785/0220200212.

Introduction

Seismic, geodetic, remote sensing, and geochemical data play a fundamental role in observing and understanding ongoing processes within active volcanic systems (Tilling, 1987) and, along with knowledge of the past volcanic behavior and suitably tailored model output (Pallister *et al.*, 2019), are critical for monitoring volcanoes and anticipating their eruptive behavior. Eruptions are commonly preceded by seismic precursors (such as seismic swarms and volcanic tremor), ground deformation, and change in gas flux and composition that can be detected and tracked continuously by means of permanent ground stations and satellite observations (e.g., Chouet and Matoza, 2013;

1. Université de Paris, Institut de Physique du Globe de Paris, CNRS, Paris, France; 2. Observatoire Volcanologique du Piton de la Fournaise, Institut de Physique du Globe de PARIS, La Plaine des Cafres, France; 3. Laboratoire Géosciences Réunion, Université de La Réunion, Saint Denis, France; 4. Now at German Research Centre for Geosciences (GFZ), Potsdam, Germany; 5. Laboratoire Magmas et Volcans, Université Clermont Auvergne, CNRS, IRD, Clermont-Ferrand, France; 6. Now at UCD School of Earth Sciences, University College Dublin, Dublin, Ireland; 7. Dipartimento di Scienze della Terra, Università di Torino, Turin, Italy; 8. Centro Interdipartimentale sui Rischi Naturali in Ambiente Montano e Collinare, Università di Torino, Turin, Italy; 9. Université Grenoble Alpes, Université Savoie Mont Blanc, CNRS, IRD, IFSTTAR, ISTerre, Grenoble, France; 10. Department of Space, Earth and Environment, Chalmers University of Technology, Gothenburg, Sweden; 11. Istituto Nazionale di Geofisica e Vulcanologia (INGV), Palermo, Italy; 12. Department of Geology and Environmental Science, University of Pittsburgh, Pittsburgh, Pennsylvania, U.S.A.

*Corresponding author: peltier@ipgp.fr

Philipson *et al.*, 2013; Biggs and Pritchard, 2017; Allstadt *et al.*, 2018). For the last few decades, the quality and quantity of data used to remotely monitor volcanoes from the field or space have increased tremendously (e.g., Ramsey and Harris, 2013; Pinel *et al.*, 2014). This allows real-time continuous data collection, 24 hr a day and 365 days a year, which is a fundamental necessity for successful volcano monitoring and eruption management. These monitoring networks must acquire and transmit the data continuously whatever the context, even during lockdown periods (including those inflicted by cyclones, national strikes, civil disorder, or epidemics). Under such conditions, movement is restricted and fieldwork is limited or impossible. The availability of reliable field and satellite data is thus crucial when a volcanic crisis is added to the context of a health crisis that both limits the mobility of observatory staff and monopolizes the work of the civil protection and the decision makers with whom they must work. Such a situation poses significant challenges but is an excellent practical test for operational volcano-monitoring networks.

The 2–6 April 2020 eruption of Piton de la Fournaise (La Réunion Island, France) occurred during the coronavirus disease 2019 (COVID-19) pandemic lockdown and presented just such a test. The lockdown took effect in France from 17 March to 11 May 2020 to counter the spread of the COVID-19 pandemic. During the lockdown period in France, as in many other countries around the world, social distancing was implemented, many workspaces were closed, telework was implemented, mobility was restricted, and other public health intervention measures were put into place, such as closure of all but essential retail outlets. The lockdown thus limited Observatoire Volcanologique du Piton de la Fournaise (OVPF) field investigations, face-to-face communications, and helicopter flights. However, continuity of operations (data acquisition, scientific, and interservice communications) was maintained due to the existence of well-established response protocols, the presence of a robust continuous real-time monitoring network, and an effective system of remote management of volcanic crises via the WebObs (Beauducel, Lafon, *et al.*, 2020) interface. In this article, we present the long- and short-term precursors to the eruption, and the evolution of the eruption recorded by the real-time monitoring data from the permanent field instruments and satellite array used by OVPF. In doing this, we show how the observatory staff remotely managed the volcano crisis with stakeholders based only on these monitoring networks and in absence of ad hoc field investigation of the eruption.

Eruption Dynamics at Piton De La Fournaise

Piton de la Fournaise is a basaltic hotspot volcano located on La Réunion (a French island in the Indian Ocean; Fig. 1a). With an average of two eruptions per year during the last 40 yr, it is among the world's most active volcanoes (e.g., Peltier *et al.*, 2009; Roult *et al.*, 2012). The majority of its recent eruptions are effusive and characterized by the opening of eruptive fissures, which feed lava fountains, strombolian activity, and lava flows (e.g., Gurioli *et al.*, 2018). More than 97% of the activity occurs inside the uninhabited Enclos Fouqué caldera (Villeneuve and Bachèlery, 2006), either at the summit or on one of its flanks, mainly on or at the base of the terminal cone, along one of the rift zones (e.g., Bachèlery, 1981; Michon *et al.*, 2007; Bonali *et al.*, 2011). The rift zones (N, S, and N120; see Fig. 1c for location) are zones of weakness and thus preferential pathways for magma to reach the surface. The 2–6 April 2020 eruption is part of a cycle involving a total of 20 eruptions as of the end of April 2020. It began in 2014 after a 41 month long period of inactivity (between 2011 and 2014; Peltier *et al.*, 2016). Like all other six eruptions that occurred in 2019 and early 2020, the 2–6 April 2020 eruption was located within the Enclos Fouqué caldera and on the N120 rift zone (see Fig. 1c for location).

Past studies suggest that most Piton de la Fournaise eruptions are fed by dikes (or sills) initiating from a shallow magma reservoir system that is located at about 2.5 ± 1 km below the summit craters (e.g., Peltier *et al.*, 2009, 2018). Eruptions are systematically preceded by three types of precursors: volcanotectonic (VT) seismicity, volcano deformation, and CO_2 soil degassing, all of which occur on two timescales. In the long-term (weeks to months), slow edifice inflation (less than 3 mm per day), increased seismicity (with 10–100 VT earthquakes per day), and enhanced soil CO_2 ground degassing (e.g., Boudoire *et al.*, 2017; Sundermeyer *et al.*, 2020) are recorded. These changes are thought to be linked to the refilling and pressurization of the shallow magmatic storage system (e.g., Peltier *et al.*, 2009, 2018). The recharging mechanism of this system has become discontinuous since 2016 (Peltier *et al.*, 2018), with periods of continuous inflation sometimes accompanied by deep seismicity (Lengliné *et al.*, 2016), interspersed with periods of no ground deformation. In the short-term (tens of minutes to hours), rapid ground deformation and swarms of shallow VT earthquakes (that are located above sea level [a.s.l.], i.e., at a depth of less than 2.5 km below the surface) are recorded. Such periods are referred by OVPF as "seismic crises" and are characterized by up to 1000 events per hour. These short-term precursors are linked to the final phase of magma injection, with magma escaping from the shallow reservoir and propagating toward the surface (e.g., Peltier *et al.*, 2009; Roult *et al.*, 2012; Duputel *et al.*, 2019). Arrival of the magma at the surface corresponds to the onset of eruptive activity and the beginning of detection of SO_2, and heat emissions as recorded by satellite-based sensors (Coppola *et al.*, 2017; Tulet *et al.*, 2017). Eruption precursors, both long- and short-term, are detected and monitored by the operational volcano-monitoring network maintained by OVPF.

The Volcano Observatory

OVPF is one of the French overseas volcano observatories managed by the Institut de Physique du Globe de Paris (IPGP). It has

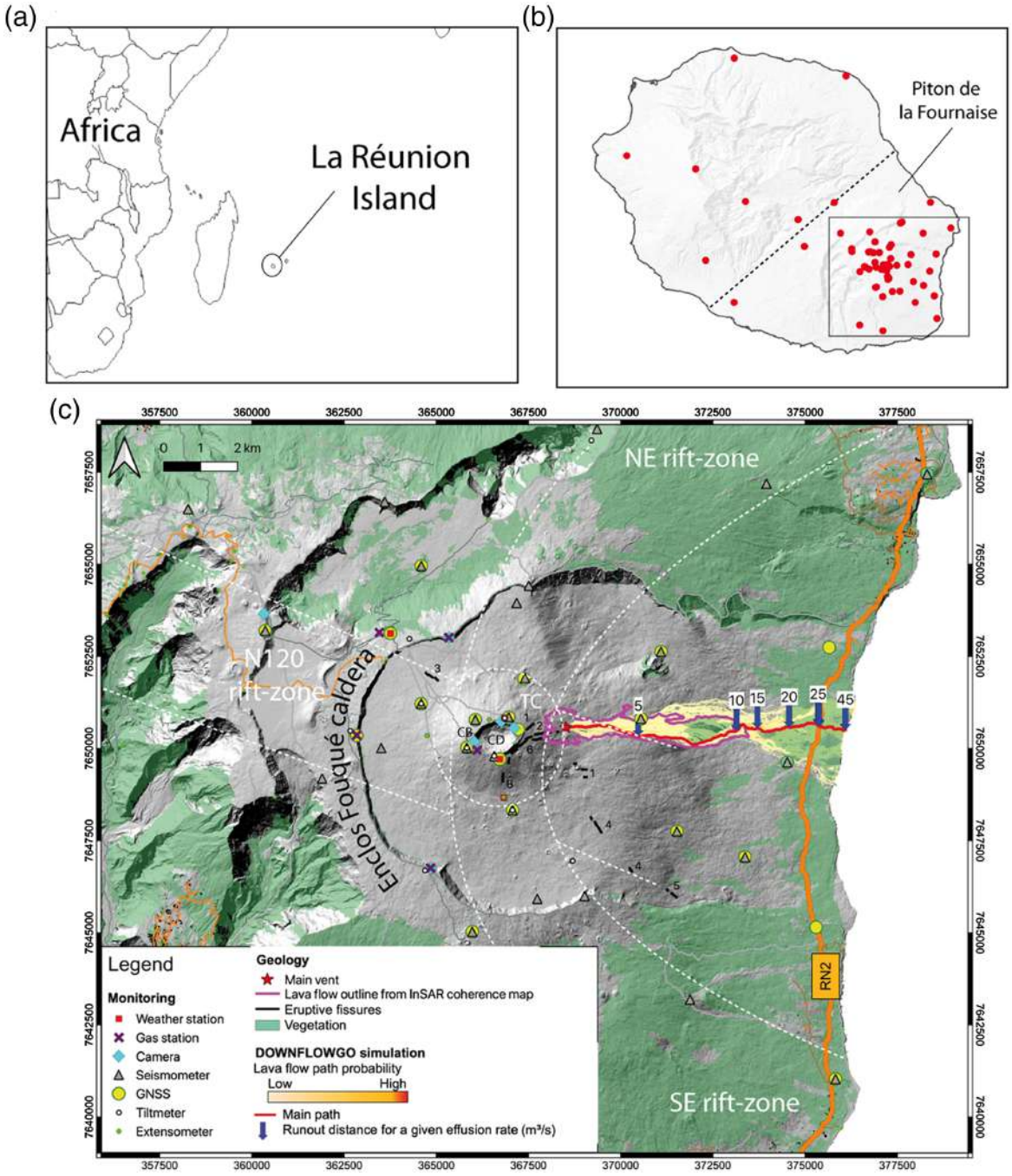

Figure 1. (a) Location of La Réunion Island in the Indian Ocean. (b) Location of the Observatoire Volcanologique du Piton de la Fournaise (OVPF) permanent monitoring stations (red dots) on La Réunion Island. (c) Zoom on the most active part of the Piton de la Fournaise volcano. Locations of the permanent monitoring stations are given as red squares: weather stations; purple crosses: gas stations; blue diamonds: cameras; gray triangles: seismometers; green circles: Global Navigation Satellite System (GNSS) receivers; white dots: tiltmeters; green dots: extensometers. The extent of the 2–6 April 2020 lava flow field mapped using Interferometric Synthetic Aperture Radar (InSAR) coherence imagery is outlined in pink. Yellow to red lines represent the frequency of probable lava flow inundation paths from low (yellow) to high (red) as computed from numerical simulations via the DOWNFLOW model of Favalli *et al.* (2005). The inundation area is computed for 10,000 iterations from the vent location with vertical elevation noise of 2 m. The line of steepest descent (LoSD) is shown in red. Blue arrows represent the location at which the lava could extend along the LoSD for given discharge rates (numbers are in m^3/s) as modeled using PyFLOWGO (Chevrel *et al.*, 2018). Black lines represent the location of the 2019–2020 eruptive fissures (numbers refer to the date of the eruption; 1: 18 February–10 March 2019, 2: 11–13 June 2019, 3: 29–30 July 2019, 4: 11–15 August 2019, 5: 25–27 October 2019, 6: 10–16 February 2020) and the red star locates the 2–6 April eruptive fissure. BC, Bory crater; DC, Dolomieu crater; TC, terminal cone. The roads and the touristic paths are in orange and gray, respectively. Coordinates are in meters (WGS84, UTM 40 S). The color version of this figure is available only in the electronic edition.

been in charge of the Piton de la Fournaise volcano monitoring since its founding in 1979 in Bourg Murat (15 km northwest of the Piton de la Fournaise summit) and assures monitoring and reporting duties to all relevant stakeholders.

Field-Monitoring Networks and Satellite Observation Services

OVPF has developed one of the densest volcano-monitoring networks in the world. The number of instruments permanently installed across the island has increased from five in 1981 (Bachèlery *et al.*, 1982) to 101 by 2020. These stations record and transmit data continuously and in real time to OVPF. Ninety-two percent of the stations are located within a radius of less than 15 km from the summit of Piton de la Fournaise (Fig. 1b). On the upper part of Piton de la Fournaise, the mean distance between stations is about 2 km. As of April 2020, OVPF maintained 41 seismometers (24 broadband three-component stations and 17 short-period sensors), 24 Global Navigation Satellite System (GNSS) receivers, 10 pairs of tiltmeters, and three extensometers (three sensors per site). In addition, eight gas stations (four stations to record CO_2 soil emissions, three Network for Observation of Volcanic and Atmospheric Change (NOVAC) (Galle *et al.*, 2010) stations to record SO_2 fluxes, and one MultiGAS station to monitor air composition at the summit), nine optical cameras, one infrared camera, and five weather stations were operational (Fig. 1c).

In addition to field instrumentation, volcano crisis management is supported by means of satellite-based monitoring. OVPF has direct access to the systems and the data of the observation services (SO) of the Observatoire de Physique du Globe de Clermont-Ferrand (OPGC) in Clermont-Ferrand (France). Specifically, Observatoire Interferometric Synthetic Aperture Radar (InSAR) de l'Océan Indien (OI^2) delivers (InSAR products, such as interferograms and coherence maps (Richter and Froger, 2020, and references therein). HOTVOLC, a web-based volcano-monitoring system that uses MSG-SEVIRI geostationary satellite data (see Data and Resources), provides real-time products including lava discharge rates, ash cloud concentration and altitude, and SO_2 dispersion maps (Guéhenneux *et al.*, 2015; Gouhier *et al.*, 2016). Since 2018, OVPF has also developed complementary Synthetic Aperture Radar (SAR) data-processing capabilities on-site, including multi-temporal InSAR (MT-InSAR) processing chains. OVPF also works with satellite data and products accessible via the MIROVA platform (University of Turin; see Data and Resources), which is a near-real-time volcanic hotspot detection and tracking system based on analysis of moderate-resolution imaging spectroradiometer data. This system allows for the estimation of time-averaged lava discharge rates (e.g., Coppola *et al.*, 2020), which are volume fluxes integrated over a period of time (Harris *et al.*, 2007). Since 2018, a multinational (OVPF-IPGP, Laboratoire Géosciene Réunion-IPGP, Université Clermont Auvergne-OPGC, University of Turin, University of Pittsburgh) satellite-data-driven protocol has been implemented to deliver near-real-time assessments of lava flow propagation at Piton de la Fournaise (Harris *et al.*, 2017, 2019; Coppola *et al.*, 2020). As a recent addition to this, the advanced spaceborne thermal emission radiometer (ASTER) Urgent Request Protocol (URP), which automatically prioritizes and targets ASTER data acquisition toward the volcanic target (Ramsey, 2016), is activated during any new eruption at Piton de la Fournaise (Harris *et al.*, 2019). As part of the Kalideos project, funded and managed by the Centre National d'Etudes Spatiales, OVPF also benefits from access to Spot 6/7, Pléiades, and TerraSAR-X data. At last, since 2014, airborne 2D and 3D mapping missions have been performed as often as possible during, and always after, each eruption.

A remotely operated 24/7 monitoring system

Within the framework of the Organisation de la Réponse de Sécurité Civile (ORSEC)—volcan du Piton de la Fournaise emergency plan, OVPF informs the civil protection department of the Préfecture (i.e., the decentralized administrative service of the French government) of any changes of volcanic activity, and advises over change the alert level when necessary. For La Réunion, this is the Etat-Major de Zone et de Protection Civile de l'Océan Indien Préfecture (EMZPCOI). The final decision regarding, and execution of, advised safety measures, as well as communication to other actors (such as town councils, the Gendarmerie (local police), central authorities, institutions, and the media) remains the sole responsibility of the Préfet (i.e., the head of the Préfecture). A rise in the alert level results in access limitations to the Enclos Fouqué caldera, flight restrictions and evacuations if needed. OVPF is also in charge of sending a Volcano Observatory Notice for Aviation to the Volcanic Ash Advisory Center in Toulouse (France) if there is any change in volcanic activity. OVPF, like all other volcano observatories in France, is part of the Service National d'Observation en Volcanologie (SNOV—National Observation Service for Volcanology). SNOV is operated by the Institut National des Sciences de l'Univers of the Centre National de la Recherche Scientifique and is in charge of scientific duties at, as well as data collection and distribution for, all active French volcanoes.

Since its foundation in 1979 through the end of April 2020, OVPF has anticipated, observed, and monitored 79 eruptions with the help of a well-established and continuously expanding volcano-monitoring network. This was possible because of OVPF's research, monitoring, and communication efforts, which are based on 24/7 operational protocols and remote accessibility to real-time data. This approach meant that the transfer to monitoring during lockdown was seamless. As part of this system, all recorded data are available online in real time to OVPF staff and collaborators through the WebObs interface (Beauducel, Lafon, *et al.*, 2020). This is a web-based tool that integrates, centralizes, processes, models, and automatically

displays data time series as well as derivative results and products (such as tremor maps, real-time seismic-amplitude measurement trends, and inverse modeling of deformation). This is coupled with an automatic alarm triggered by preset thresholds for key monitoring stations and activity signals. This alerts the duty scientist in case of a change in the recorded signals. Normal operations included in the internal OVPF duty protocol ensure that OVPF staff members alternate in keeping watch over the volcanic activity and of the proper functioning of the entire operational chain, with daily checks being made every morning, each duty scientist having a shift of 7 days. During eruptions, duty protocols are reinforced and a routine manual check for the continuity of data acquisition and the volcano's eruptive behavior is added, in which the check is made every 3 hr (during days and nights, with shifts of 6–12 hr). In case of any change in activity, the director (Scientist-in-Charge) of OVPF is informed and information is relayed to EMZPCOI.

The 2–6 April 2020 Volcano Crisis at Piton De La Fournaise

Eruption precursors

The 2–6 April event was preceded by both long- and short-term precursors, which were recorded by the OVPF networks and fell within the characteristic pattern observed for Piton de la Fournaise eruptions.

Long-term observations. The 2–6 April eruption was preceded by very low-intensity, long-term geophysical precursors that started on 29 March, four days prior to the onset of the eruption. Seismicity levels below the summit craters increased from 1, through 3 and 7, to 12 shallow VT earthquakes per day on 29, 30, 31 March and 1 April, respectively (Fig. 2a). Epicenters were located between 1.5 and 2.5 km below the Dolomieu crater (Fig. 2e). Over the same period, inflation (an increase of 1.5 cm in distance between two GNSS stations that are located at opposite sides of the terminal cone) also renewed after a 19 day pause (Fig. 2c). This small amount of deformation can be modeled in real time using an unsupervised inverse problem and a compound dislocation model source (Nikkhoo *et al.*, 2017; Beauducel, Peltier, *et al.*, 2020). On 1 April, the pre-eruptive inflation was interpreted as being due to pressurization of a single source: an ellipsoid with a volume increase of 450,000 ± 50,000 m^3 located at about 1 km below the Dolomieu crater (Fig. 2d). In addition, the soil CO_2 flux, that had shown an increasing trend between early December 2019 and 9 February 2020, just before the 10–16 February, eruption, began to increase again, albeit slowly, from 1 March, but then quickly from 27 March (Fig. 2b). This pulsatory behavior in soil CO_2 fluxes records the ascent of volatile-rich magmatic fluids from the deepest part of the volcano's plumbing system (Boudoire *et al.*, 2017) and produced the pressurization of the shallow reservoir recorded by the geophysical networks.

Short-term observations. After only four days of increased seismicity and edifice inflation, a seismic crisis began on 2 April, at 04:15 UTC (Fig. 3a), indicating that magma had escaped from the shallow reservoir and had begun propagating toward the surface. A total of 92 shallow VT earthquakes were recorded below the summit between 04:15 and 04:51 UTC. They were located mainly between 1.5 and 2.5 km below the southeastern part of the Dolomieu crater. This seismic crisis was accompanied by rapid surface inflation, but of very-low amplitude (<10 cm; Fig. 3c).

The seismic crisis was characterized by a low number of events compared with previous swarms at Piton de la Fournaise during which up to 1000 earthquakes per hour can be recorded (Duputel *et al.*, 2019). In addition, the associated surface inflation was very small in magnitude (i.e., less than 10 cm of uplift that was confined to the very proximity of the eruptive fissure; Fig. 3c). These observations suggest that the magma followed pre-existing pathways at depth, using pathways opened during previous eruptions in 2019 and 2020, opening in approximately the same area as the April 2020 eruption, that is, intrusion below the southeastern part of the Dolomieu crater with vent opening on the eastern flank (Fig. 1c).

The eruption

The signs of continuous seismic tremor at frequencies between 0.5 and 5 Hz provide evidence that magma is at or very close to the surface (e.g., Chouet, 1996). Eruption tremor is a continuous ground vibration that has been systematically recorded during eruptions at Piton de la Fournaise (e.g., Battaglia *et al.*, 2005; Journeau *et al.*, 2020). Tremor first appeared on the OVPF seismic network around 08:20 UTC on 2 April (Figs. 3a and 4b). This allowed the eruptive vent to be located on the eastern flank, close to one of the OVPF ground stations (FLR; Fig. 3b). Between 10:35 and 10:45 UTC, a thermal anomaly was detected by the MIROVA and HOTVOLC systems, which confirmed the presence of lava at the surface. It also allowed a first estimation of the discharge rate (Fig. 4f) and triggered the ASTER URP system, scheduling an ASTER observation at the next possible overpass. In spite of the lockdown, an overflight was undertaken by Gendarmerie 2.5 hr after the beginning of the eruption and confirmed that a single fissure had opened on the eastern flank of the terminal cone, in direct continuity of those that were activated during the 10–16 February 2020 eruption (Fig. 1c). Surface deformation patterns (Fig. 3c) and average vertical amplitudes across the seismic array (Fig. 4b) did not indicate further subsurface propagation of magma. This gave reasonable certainty that the intrusion would not propagate beyond the eruptive fissure so as to open at lower elevations (and potentially threaten the island belt road RN2, Fig. 1c), or outside of the Enclos Fouqué caldera so as to impact populated areas.

Seismicity started to increase on 4 April and continued until 6 April. Events were located at 1.3–4 km below the

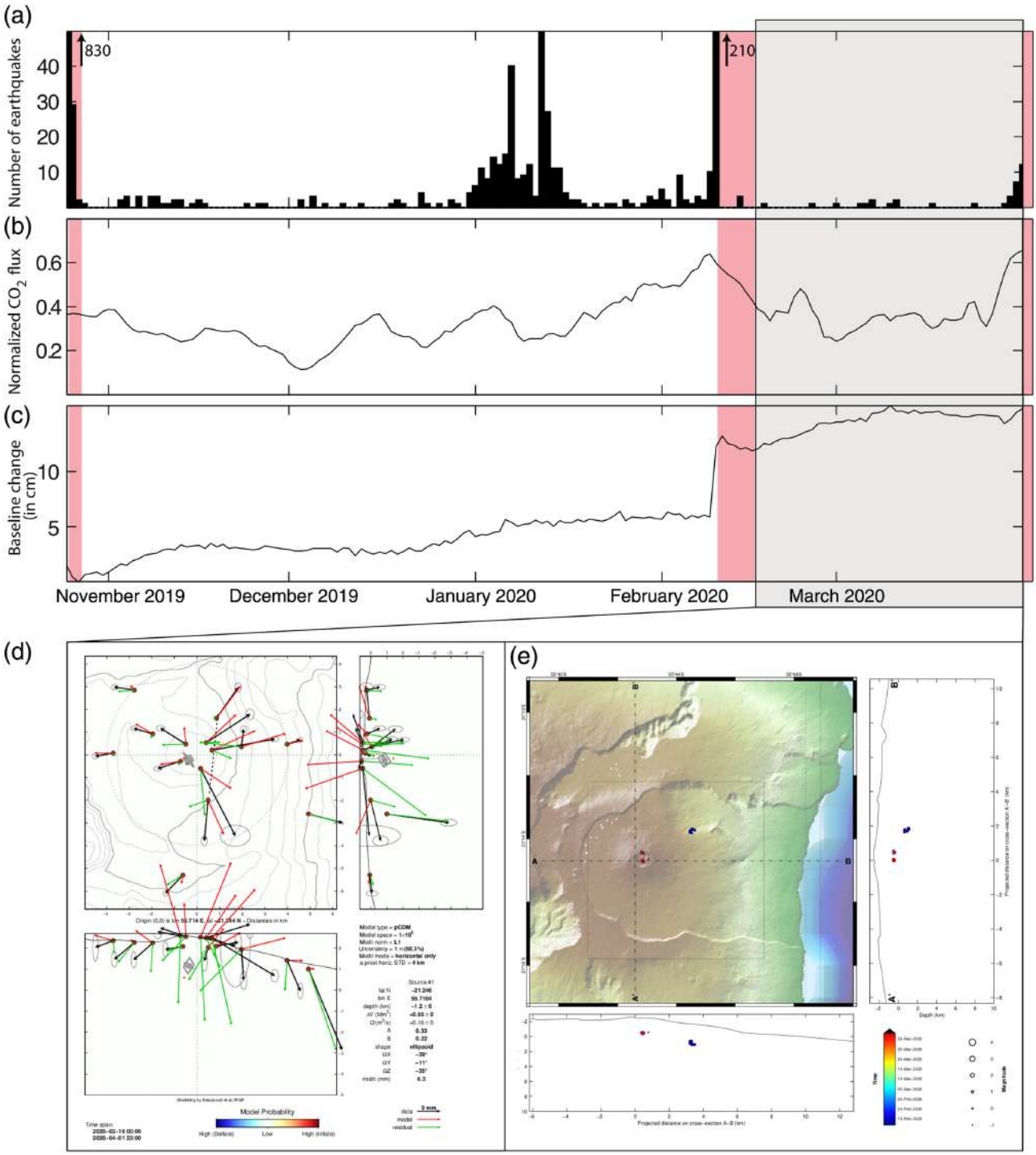

Figure 2. Long-term precursors preceding the 2–6 April 2020 eruption. (a) Number of shallow volcanotectonic earthquakes per day. (b) Normalized soil CO_2 flux from distal stations. (c) Summit deformation as recorded by GNSS baseline variation (baseline is shown by the dotted line in panel (d)). Red bars mark the eruptive periods. (d) point compound dislocation model (pCDM) source solution from Bayesian inversion of the displacement trends preceding the eruption (from 17 February, i.e., the end of the previous eruption, to 1 April) in map and vertical cross-section views. Color map indicates the maximum probability combined with volume variation sign (yellow–orange–red for inflation). Black, red, and green arrows are observed displacements, modeled displacements, and residual, respectively. Ellipses are errors for the observed displacements. Best model sources are indicated as gray planes. (e) Location map (epicenters) and north–south and east–west cross-sections (hypocenters) of earthquakes at Piton de la Fournaise as recorded between 17 February and 1 April. Only locatable earthquakes are shown on the map, although the observatory records more seismic events that are not locatable due to their small magnitude. The color version of this figure is available only in the electronic edition.

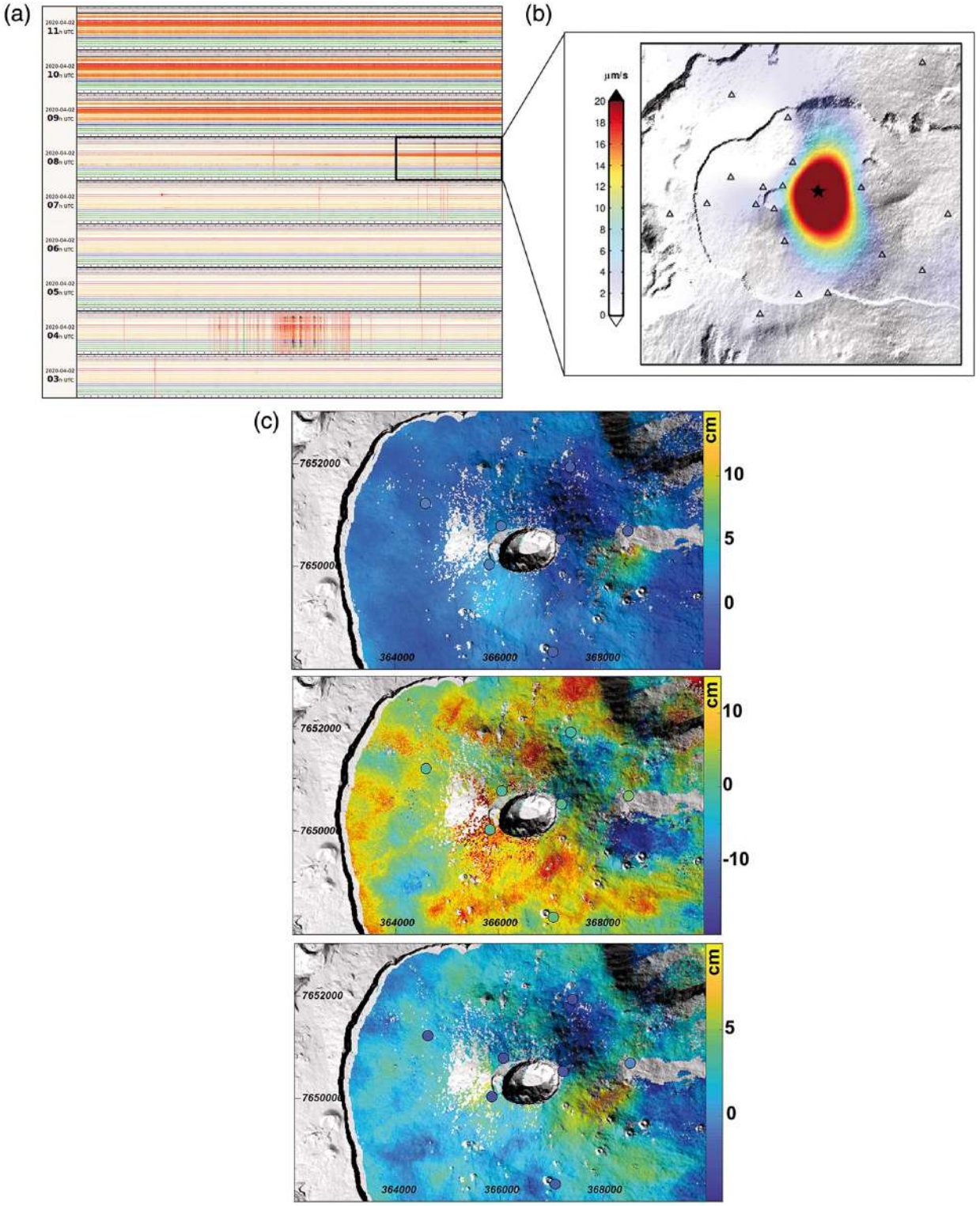

Figure 3. Short-term precursors preceding the 2–6 April 2020 eruption. (a) Seismic signals recorded on the vertical component of 19 stations of the OVPF network between 03:00 UTC and 11:59 UTC on 2 April for each hour (as indicated by the time step on the *y* axis, in which time increases toward the right). Each red vertical bar represents an earthquake. Note the appearance of the tremor at 08:20 UTC. (b) Tremor map computed for the 08:45–09:00 period. (c) Maps of east–west (top), north–south (middle), and vertical (bottom) displacements, associated with the 2–6 April 2020 eruption calculated from Sentinel-1, PAZ, and Advanced Land Observation Satellite (ALOS2) interferometric data. Filled circles represent displacements recorded on the OVPF permanent GNSS stations. Intensity of the displacements is given by the colored bar. The color version of this figure is available only in the electronic edition.

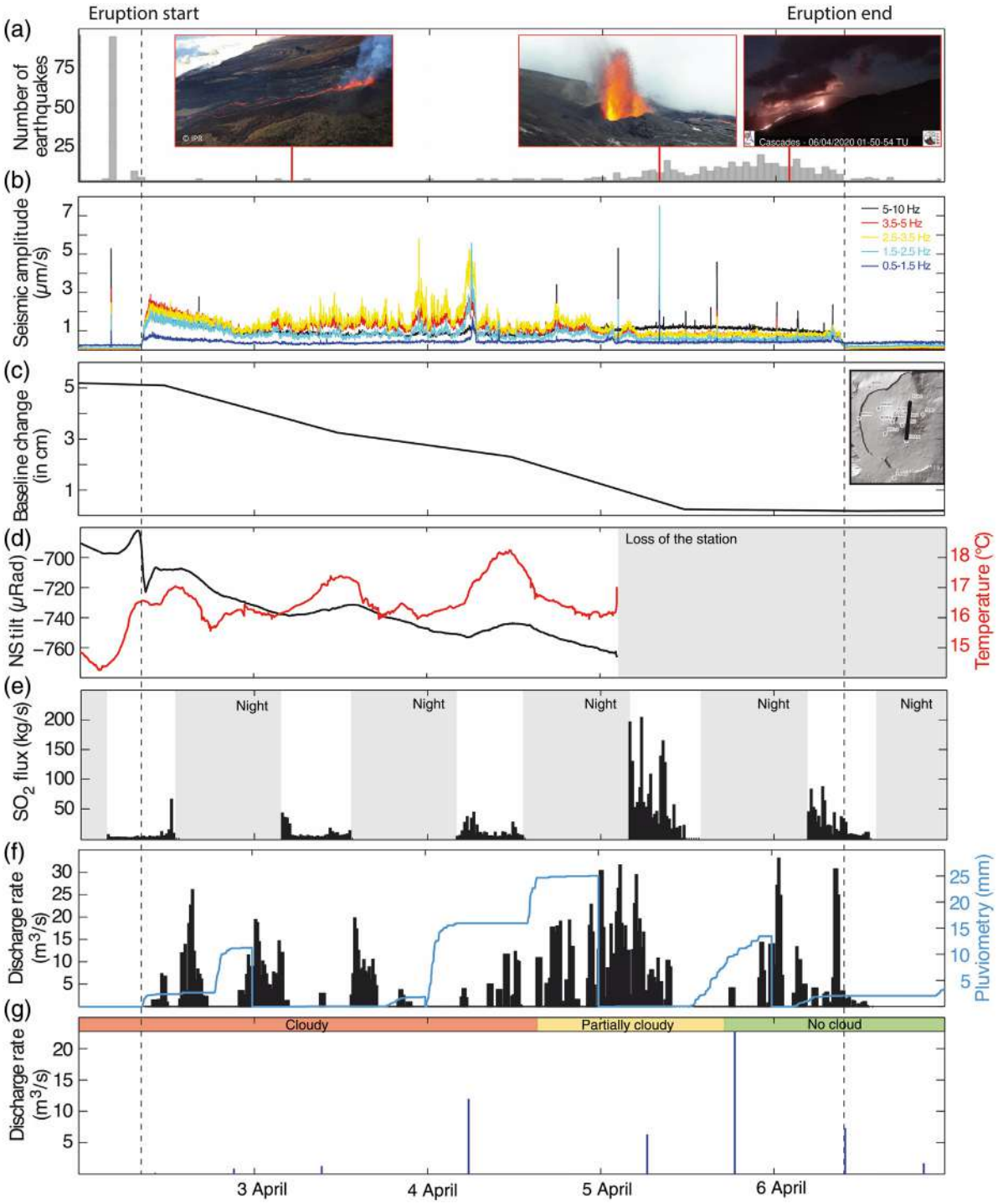

Figure 4. Geophysical and geochemical trends during the 2–6 April 2020 eruption. (a) Number of shallow volcanotectonic earthquakes per hour. Insets: aerial photographs taken on 3 April (Imaz Press Réunion) and 5 April (SAG-PGHM), and from the "Cascades" OVPF ground webcam on 6 April. (b) Average amplitudes of the vertical component of the FJS OVPF seismic station, located 1.7 km northwest of the eruptive site, in different frequency bands. The signals are filtered, and the average amplitude is calculated over 1 min. (c) Summit deformation as recorded by a GNSS baseline variation. Inset: location of the baseline. (d) Tilt (in black) and air temperature (in red) recorded on the north–south direction on the FLR station, located 200 m from the eruptive fissure. (e) SO_2 flux measured by the PARN NOVAC station located at 4 km northwest of the eruptive site. (f) Discharge rates (black bars) estimated by the HOTVOLC platform and daily cumulative rainfall (in blue) recorded at the summit by the SFRI OVPF pluviometer. (g) Discharge rates (blue bars) estimated by the MIROVA platform. Heavy cloud cover prevented accurate estimate of discharge rates during much of the eruption, during which absolute values and trends are unreliable due to variable degrees of cloud cover. The color version of this figure is available only in the electronic edition.

southeastern sector of the Dolomieu crater, with 12 earthquakes on 4 April, 164 earthquakes on 5 April, and 91 earthquakes on 6 April (Fig. 4a). This seismicity was accompanied by a low-magnitude deflationary trend (summit contraction of <5.5 cm; Fig. 4c). These signals were interpreted as signs of rapid emptying of the shallow magmatic reservoir below the Dolomieu crater. All the same, a continuous increase in soil CO_2 fluxes (which continued throughout the eruption, even if at a slower rate with respect to the pre-eruptive phase) suggested a continuous deep magma influx into the shallow reservoir.

Simultaneous with the increase in seismicity, the eruptive activity at the vent increased (Fig. 4f,g). Discharge rates estimated via HOTVOLC and MIROVA were, unfortunately, compromised by increased amounts of cloud cover (as revealed by the rainfall data in Fig. 4g), which contaminated measurements at the beginning of the eruption and during 4–5 April (Fig. 4f). However, peaks in HOTVOLC and MIROVA time series during cloud-free windows gave values of around 30 m^3/s. The mean effusion rate over the entire eruption period, however, has been estimated at 16 m^3/s (Fig. 4f).

Following the increase of eruptive activity, OVPF lost signals from one station, FLR, which was located at about 150–200 m from the eruptive site, on 5 April at 02:22 UTC. A close observation of the seismic data recorded by this station just prior to losing the signal shows a vertical uplift of the station at 02:12, 02:13, and 02:14 UTC, simultaneous with a low-frequency peak at other stations of the network (0.5–1.5 Hz; Fig. 4b). This could suggest a pressure increase before the opening of a second fissure near the FLR station. Tiltmeter data support this hypothesis with a rapid tilt to the south and a gradual increase in the air temperature directly before loss of the signal (Fig. 4d). In addition, a particularly high discharge rate of 31.5 m^3/s was recorded by HOTVOLC at 03:00 UTC, around 40 min after the loss of the station (Fig. 4f). This, too, is compatible with opening of a second vent and a new phase of fountain-fed lava flows. On 5 April, during an overflight that was undertaken by Gendarmerie 4 hr after the loss of the signal, lava fountains were estimated as exceeding 50 m in height. Because of unfavorable weather conditions, a dedicated flight maneuver to closely investigate the situation at the FLR station was not possible. It was also impossible to confirm whether the active fissure was a new one, close to the first one, because the landscape had changed too much since the previous overflight due to emplacement of new lava flows and growth of cinder cones (Fig. 4a).

During the most intense phase of the eruption (i.e., between 5 and 6 April), a significant amount of Pele's hair was emitted. Pele's hair is thin, elongated, and sharp volcanic glass fibers that form during phases of strong degassing and high eruption rate fountaining (Thivet *et al.*, 2020). They are fluid ejections that are stretched during their flight into thin strands (Moune *et al.*, 2007). During that time, NOVAC scans of the volcanic plume consisting of gas and small particles constrained its height to approximately 4040 ± 150 m a.s.l. (i.e., ~1.4 km above the volcano summit). Strong winds caused these plainly very aerodynamic and relatively sparse filaments to be transported over unusually long distances, being deposited over almost all of the islands (found up to 50 km from the vent).

5 and 6 April clearly marked the highest-intensity phase of this eruption, characterized by high lava discharge rates (Fig. 4f,g), strong seismicity (Fig. 4a), edifice deflation (Fig. 4c), high CO_2 flux, the formation of Pele's hair in large quantities, and an increase in SO_2 flux with respect to the first days of the eruption (Fig. 4e).

The eruption stopped abruptly on 6 April 2020 at around 09:30 UTC and after a rapid decrease in the tremor (Fig. 4b). A similar pattern has been observed for about half of all monitored Piton de la Fournaise eruptions. Considering the areal coverage of the associated lava flow estimated from the InSAR coherence map (Fig. 1c, 3.3×10^6 m^2), and under the assumption of an average thickness of 2–3 m (which is the average value observed for Piton de la Fournaise lava flows), we estimated a total erupted bulk lava volume of the 2–6 April eruption of $6–10 \times 10^6$ m^3. As a comparison, the total lava volume calculated from integrating the discharge rates obtained from the MSG-SEVIRI data through time (Fig. 4f) gives a total volume of erupted lava of 5.4×10^6 m^3. However, this value is likely to be an underestimate due to cloud cover during the eruption. Given the eruption duration of around 95 hr, these total volumes give a mean output rate of lava over the entire eruption period of between 16 and 29 m^3/s.

Because of orbital constraints, the first ASTER daytime scene was acquired on 7 April, only five days after the URP system was triggered. This is a significant improvement to the standard 16 day repeat time of ASTER, but unfortunately the eruption had ended by this time and the island completely cloud covered. ASTER acquisitions continued until 12 April in an attempt to acquire a cloud-free image to check if the air fall Pele's hair had had any effect on vegetation health, through use of the normalized vegetation index capability of ASTER (Hulley *et al.*, 2015), but acquisitions continued to be hampered by cloud cover. A field investigation by an OVPF team on 9 April could not fully clarify whether a second fissure had opened close to the first one because a large 300 m wide cone had formed by tephra accumulation, thereby burying any field evidence. An extensive fallout zone of scoria was observed around the eruptive cone with tephra deposit thicknesses greater than 1 cm extending 400–500 m around the vent (Fig. 5a). However, we were able to confirm that paroxysmal activity at the end of the eruption had buried the FLR station (Fig. 5b). The base of the 2–6 April eruptive cone was less than 20 m from the former FLR station location. This station was equipped with one seismometer, one GNSS sensor, a pair of tiltmeters, and one rain gauge, resulting in a total monetary loss of approximately 30 k€.

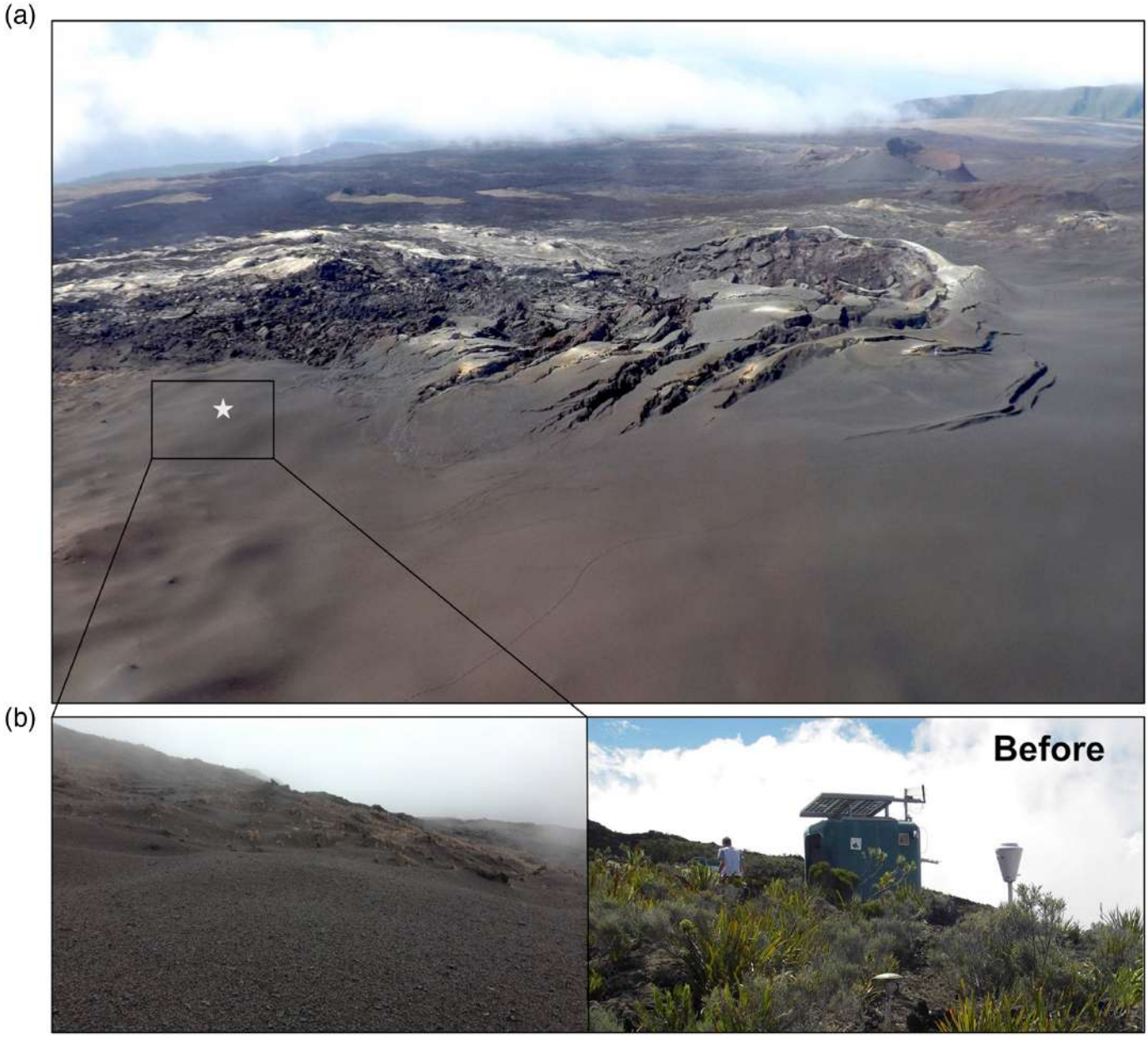

Figure 5. (a) Photograph of the eruptive site taken after the eruption on 11 May 2020. The white star shows the buried location of the FLR station. (b) The site of the FLR station before (right) and after (left; on 9 April 2020) the eruption. The color version of this figure is available only in the electronic edition.

Eruption management during lockdown

Because of the COVID-19 lockdown, the OVPF staff worked remotely from home during the period of precursory unrest that began at the end of March. Upon the announcement of lockdown, a reduced activity plan was set up to maintain remote monitoring operations and to authorize fieldwork when absolutely necessary, for instance, to repair a monitoring station or transmission relay upon loss of signal. Urgent maintenance was thus still possible, if needed, to ensure continuous and effective monitoring. Similarly, additional field operations were only permitted when or if property or population were threatened by an eruption. The OVPF technical service implemented a set of solutions to facilitate telecommuting, including use of a broadband virtual private network to allow the staff to continue to use the observatory IT resources, allowing remote access to essential services such as processing servers, network storage, and data-processing software.

In response to precursory signals recorded by the monitoring networks during the four days before the start of the eruption, the OVPF director informed EMZPCOI about the renewal of reservoir pressurization (Fig. 2). On 2 April, at the beginning of the seismic crisis (i.e., at 04:15 UTC; Fig. 3a), the duty scientist received an automatic alarm via cell phone. This

had been initiated by the tripping of thresholds at several seismic-monitoring stations. This was followed by immediate notification of the OVPF director and the full OVPF scientific team that an eruption was imminent. Following the standard OVPF protocol, the OVPF director then called EMZPCOI, and the Préfecture triggered the ORSEC – volcan du Piton de la Fournaise emergency plan. During these phases of eruption response, none of the OVPF-EMZPCOI–Préfecture communications require face-to-face meetings, which are only organized when imminent eruptions pose a direct threat to public safety or property. Following this first communication phase, the Préfecture raised the level to "Alert 1: imminent eruption." The only difference between normal times was that, because of the lockdown, the hiking trails were already closed and tourist activities were prohibited, so no evacuation from the Enclos Fouqué caldera (Fig. 1c) was necessary.

Regarding the scientific interactions within the OVPF team, no meeting in the crisis room in front of the observatory's control screens was possible, as is usually done during eruptive crises under normal conditions. Instead, the "crisis meeting" was organized online and a dedicated dialog room was created to remotely manage the crisis and ensure efficient communication, data analysis, sharing, and brainstorming among all staff members, all of whom had real-time access to all data through the online WebObs monitoring tool.

During the first 4 hr of the seismic crisis, the OVPF staff kept EMZPCOI informed about the situation and magma propagation at depth in real time. At the first appearance of tremor on the seismic recordings at 08:20 UTC (Fig. 3a,b), OVPF informed EMZPCOI, and the Préfecture further raised the alert level status to "Alert 2-2: ongoing eruption inside the Enclos Fouqué caldera." With the beginning of the eruption, the on-call crisis procedure was activated at OVPF. Simultaneously, a helicopter reconnaissance flight was organized. This is operated by the Gendarmerie and, in normal times, the OVPF director, or an authorized OVPF staff member, joins the flight to allow a first visual observation of the eruption. However, because of the COVID-19 lockdown, no OVPF staff member was allowed aboard the Gendarmerie helicopter. Instead, remote communication between the OVPF director and a member of the helicopter team was kept open at all times. The tremor location enabled the OVPF director to coordinate and remotely guide the aerial reconnaissance in real time by text messages and phone communications. The helicopter team identified and confirmed the exact location of the eruptive site.

From the beginning of the eruption, the most probable lava flow path was modeled (Fig. 1c) using the near-real-time assessment of lava flow propagation protocol (Harris *et al.*, 2017). This protocol facilitated gathering all necessary source terms (i.e., discharge rate and fissure location) needed to model the lava flow propagation (Harris *et al.*, 2019). The resulting map of probable lava flow inundation paths was communicated to the EMZPCOI–Préfecture to assist crisis response operations. The probable lava flow inundation paths usually provide a trustworthy estimation of the final lava flow dimensions, and allowed the EMZPCOI–Préfecture to assess the risks of fires in the vegetated areas at lower elevations, as well as the likelihood of lava flow inundation of the coastal road and the threat to OVPF monitoring stations.

In the absence of in situ field investigations, real-time data received from the ground-based monitoring network, and complementary satellite observations (in particular for the discharge rates), allowed for remote detection of the paroxysmal activity toward the end of the eruption (Fig. 4). This justified a second helicopter flight undertaken by Gendarmerie and guided by OVPF on 5 April (Fig. 4a). To map the exceptionally large amount of Pele's hair fallout associated with the high discharge rates recorded at the end of the eruption, OVPF opened a call for participatory science on its social-media channels asking the population to report whether (and how much) Pele's hair fell in their gardens or on their balconies. As a result of the lockdown, everyone was at home and OVPF received about 150 testimonies in 24 hr. These were used to map the island-wide dispersion of Pele's hair (see OVPF monthly bulletin of April 2020, ISSN: 2610-5101). The resulting map was sent to the Préfecture within 48 hr after the initial call to the population and open data access was guaranteed using the DynVolc OPGC portal (see Data and Resources; Gurioli *et al.*, 2018).

Under the circumstances of the ongoing COVID-19 pandemic (as of early May 2020), co- and posteruption aerial photographs allowing a 3D reconstruction of the lava flow could not be acquired. However, the "Cascade" OVPF webcam located on the southeastern coast (Fig. 4a) permitted the evolution of the lava front propagation to be followed. Tracking of the flow front position was supported during the paroxysmal phase by field measurements from the road on the eastern coast, via a thermal infrared (FLIR) camera. This has been made by an OVPF team during the night of 5 and 6 April, in which the increase in activity meant that "property or population were threatened by an eruption," in this case potential cutting of the belt road, which is the only link between the north and south of the island on the east coast (Fig. 1c). As a result, permission for field operations was granted. In addition, coherence maps derived from MT-InSAR images allowed retrieval of the extent of the areas affected by lava flows and scoria deposits (Fig. 1c).

For any eruption (under normal or lockdown conditions), OVPF prepares a detailed activity report (in addition to the daily automatic bulletins), which is sent to EMZPCOI–Préfecture. This is sent whenever important changes in volcanic activity occurred, or at the end of the day (even if no major change in activity occurred). The bulletin is then published via the OVPF website (see Data and Resources) and distributed through the OVPF social-media channels to keep the public informed (see Data and Resources).

On 9 April, after the end of the eruption and under special authorization to allow fieldwork during lockdown as granted by the Préfecture and the IPGP scientific head, a first field reconnaissance was carried out by OVPF. This mission was carried out to repair a monitoring station at the summit, to clean solar panels covered by Pele's hair fallout, to sample the eruptive products, and to check the state of the FLR station that was knocked out during the eruption.

Discussion and Conclusions

The lockdown related to the COVID-19 pandemic considerably changed and slowed down all OVPF operations for almost two months (17 March–11 May 2020). During this time, the observatory was closed and maintenance for instrumental networks in the field was limited to urgent operations only. The closure of the observatory over such a long period is exceptional in its history. In the past, the observatory was closed only once during an eruption, for only a few hours, during a red alert due to passage of a cyclone on 15 February 2000. By 2000, remote monitoring using frequently updated satellite data was already being established (e.g., Harris *et al.*, 2000, 2001) allowing volcanic activity to be tracked remotely from anywhere (e.g., Mouginis-Mark *et al.*, 2000; Roach *et al.*, 2001). Since that time, such remote monitoring platforms have been developed further and convolved with observatory operations at OVPF (Gouhier *et al.*, 2016; Harris *et al.*, 2017), and field networks of continuously recorded geophysical instruments can be delivered over the Internet in real time via the online monitoring platform WebObs (Beauducel, Lafon, *et al.*, 2020). Therefore, remote crisis management is much easier today than it was in 2000, as exemplified by the 2–6 April 2020 eruption of Piton de la Fournaise.

Over the past 40 yr, only exceptionally short eruptions at Piton de la Fournaise, and eruptions that occurred during very unfavorable weather conditions, were not tracked using syneruptive field investigations. The April 2020 eruption is the first eruption since 1980 in which no fieldwork at the eruptive site was possible, even though the eruption location, duration, and weather conditions were suitable for such activities. The lockdown put the reliability and accuracy of real-time monitoring, remote communication and operation protocols, and effective collaboration among numerous partner institutions involved in monitoring Piton de la Fournaise to the test. Because of rapid data availability and efficient information flow, both of which are of crucial importance for a scientific crisis response, monitoring of the April 2020 eruption of Piton de la Fournaise was not just possible but was highly successful. This, in a large part, was because all remote monitoring networks and protocols have been put in place, tested, and validated before the need to apply the approach under lockdown conditions.

With 40 yr of experience and a well-developed instrumentation network, the OVPF team could efficiently manage the 2–6 April crisis despite the difficult circumstances related to the COVID-19 lockdown. Under normal circumstances, remote crisis management is a routine only employed during weekends, holidays, and at night. The only difference during the COVID-19 lockdown was that remote crisis management from home continued throughout the entire eruption. The OVPF staff is thus well experienced in remote eruption management and had already developed suitable tools to allow real-time situation analysis, such as the WebObs online monitoring tool (Beauducel, Lafon, *et al.*, 2020). Furthermore, communication with stakeholders had been optimized over the years, resulting in the development of a dedicated protocol (i.e., through notably the emergency ORSEC plan) ensuring an efficient emergency response chain and decision making. As described here, this could all be transferred seamlessly to monitoring the precursors to, and then activity during, an eruption under lockdown.

Only the experience of having to monitor an eruptive crisis without any ad hoc or on-site measurements, which are usually carried out to check and validate signals and trends apparent in data from the ground- and space-based monitoring network, was a new test. It has long been an argument that satellite-based remote sensing allows monitoring of all subareal volcanoes, providing access to eruption sites that are inaccessible from the ground due to remoteness, hazard, or difficulty of access, with the synoptic capability and repeat coverage guaranteeing that entire volcanoes are measured on a regular basis (Francis, 1979; Mouginis-Mark *et al.*, 1989; Rothery, 1992). As a result, satellite observation systems have been designed to assist crisis management at remote, poorly equipped locations, or unmonitored locations (e.g., Harris *et al.*, 2000; Mouginis-Mark *et al.*, 2000; Roach *et al.*, 2001). Our case study adds a new example to the power of measurements from in-orbit sensors to monitoring volcanic eruptions for which access is limited, here due to a lockdown associated with a global pandemic.

Similarly, OVPF's ground-based network was suitably mature and robust to allow accurate tracking of the eruptive crisis. For the 2–6 April 2020 eruption, the dense OVPF instrumentation network allowed detection, tracking, and interpretation even of the rather weak long- and short-term precursory signals. Imminent volcanic unrest was then communicated efficiently to decision-makers and local authorities using a tried and tested call down procedure. Moreover, even changes in eruptive activity, such as the paroxysmal activity toward the end of the eruption, could be recognized and followed despite the loss of the nearest monitoring station. This stresses the necessity of the need for installation and testing of a dense, resilient monitoring network, prior to a crisis, for successful crisis management, especially in situations in which field investigations are impossible. Total reliability on a largely autonomous monitoring network requires a sufficient number of ground stations, as well as an operational data transmission chain from the field to the observatory. As shown here, in such

a situation, the loss of one station is not critical for efficient monitoring of an eruption, provided functioning network of a sufficiently dense instrument array is in place. In such a scenario, failure of a data transmission relay becomes critical, as this can break the data stream continuity. For example, on New Year's Eve (31 December) in 2005 (during an eruption), heavy thunderstorms damaged a transmission relay and data were no longer transmitted to OVPF. The observatory staff was therefore blind to what was happening on the ground for a few hours while the situation was being repaired. Since that time, OVPF has developed several, partially redundant relays, so that data pass through different relays, and in the case of failure of one data reception is still assured.

OVPF can now also rely on increasing volumes of satellite data, as more missions are launched and new technologies, such as greatly improved TIR resolution, become developed, greatly increasing the availability and variety of satellite data. Such satellite constellations will be particularly useful in the unlikely event of a total ground network failure. Even at well-equipped volcanoes, such as Piton de la Fournaise, improved spatial, spectral, and temporal resolutions of satellite data will allow for the prompt recognition and quantification of critical monitoring parameters, such as pre-eruption thermal changes, discharge rate trends, lava area and volume mapping, ground deformation, and gas and ash plume dispersal. These measurements are complementary to the data delivered by ground-monitoring systems (e.g., Roach *et al.*, 2001; Peltier *et al.*, 2017; Poland *et al.*, 2020) and can be especially important linking trends from ground-based and satellite-flown instrumentation in absence of field observations, or filling gaps in coverage. This was clearly demonstrated, for example, by the co-eruptive displacement maps produced from SAR data (Fig. 3c). The displacement pattern mapped using SAR interferometry was rather weak in magnitude and limited to the immediate surroundings of the eruptive vent. No GNSS station was located within this displacement pattern. Hence, without satellite observations, this displacement would have been completely unnoticed. Vice versa, the pre-eruptive inflation in the four days prior to the eruption recorded by the GNSS stations was too weak to be detected by InSAR.

Remote volcanic crisis management is particularly important not only at volcanoes lacking an observatory, but also at well-equipped volcanoes in which access is temporarily hampered or disabled. Such factors include, for example, cyclones and blizzards, or national strikes, civil disorder, wars, or pandemics. In this regard, the global impact of the COVID-19 pandemic was unprecedented. The related lockdown in France forced remote monitoring and management of the 2–6 April 2020 eruption of Piton de la Fournaise. This posed a challenge to the volcano observatory's capacity to manage a volcanic crisis and posed a rather unique and new consideration for inclusion in best practice-based operational protocols (Pallister *et al.*, 2019). However, due to the existence of a comprehensive and fully functioning monitoring, transmission, and communication network along with a well-defined crisis management protocol, monitoring of this eruption went smoothly. Similar networks and protocols also exist at the other IPGP volcano observatories, which monitored volcano and seismic activity on two islands of the Lesser Antilles (Observatoire Volcanologique et Sismologique de Guadeloupe and Observatoire Volcanologique et Sismologique de Martinique), and on Mayotte (REseau de surveillance VOlcanologique et SIsmologique de MAyotte), which also belong to the French overseas territories. Many volcano observatories worldwide follow comparable procedures, and those can hopefully benefit from our presumably rather unusual (even unique) experience of having to respond to an eruption during the COVID-19 lockdown. Although this put our monitoring capacities and communication strategies to the test, we passed due to the seamless transition of our monitoring strategies and protocols from normal to lockdown conditions.

Data and Resources

Ground data used for this study were acquired by the Observatoire Volcanologique du Piton de la Fournais–Institut de Physique du Globe de Paris (OVPF-IPGP). All OVPF data are available upon request and data from the permanent seismic and Global Navigation Satellite System (GNSS) monitoring network can be downloaded from the IPGP Data Center (http://volobsis.ipgp.fr/). Data on Pele's hair dispersion are available on the Observatoire de Physique du Globe de Clermont-Ferrand (OPGC) DynVolc portal (http://wwwobs.univ-bpclermont.fr/SO/televolc/dynvolc/). The WebObs system is available at https://github.com/IPGP/webobs repository. MSG-SEVIRI data were acquired and processed by OPGC and accessible on the HOTVOLC website (https://wwwobs.univ-bpclermont.fr/SO/televolc/hotvolc/), and moderate-resolution imaging spectroradiometer (MODIS) data by the University of Turin are accessible on the MIROVA website (https://www.mirovaweb.it/). All ASTER data are accessible via the Land Processes Distributed Active Archive Center (LP DAAC) EarthData site (https://earthdata.nasa.gov/eosdis/daacs/lpdaac). The information about the bulletins published via OVPF is available at http://www.ipgp.fr/fr/ovpf/actualites-ovpf. In addition, the bulletins are made available to the public through OVPF social-media channels (https://twitter.com/obsfournaise; https://www.facebook.com/ObsVolcanoPitonFournaise/). All websites were last accessed in October 2020.

Acknowledgments

Observatoire Volcanologique du Piton de la Fournaise–Institut de Physique du Globe de Paris (OVPF-IPGP) operations and equipment are funded by Institut National des Sciences de l'Univers-Centre National de la Recherche Scientifique (INSU-CNRS), Ministère français de l'Enseignement supérieur, de la Recherche et de l'Innovation (MESRI), Préfecture de La Réunion, and Région La Réunion, and the lava flow simulation protocol was funded by Lava Advance into Vulnerable Areas (ANR LAVA), ANR-16 CE39-550 0009 (ANR-LAVA publication 15). The authors thank two anonymous reviewers for their helpful comments. This is IPGP Contribution Number 4165.

References

Allstadt, K. A., R. S. Matoza, A. B. Lockhart, S. C. Moran, J. Caplan-Auerbach, M. M. Haney, W. A. Thelen, and S. D. Malone (2018). Seismic and acoustic signatures of surficial mass movements at volcanoes, *J. Volcanol. Geoth. Res.* **364,** 76–106.

Bachèlery, P. (1981). Le Piton de la Fournaise (Ile de La Réunion). Etude volcanologique, structural et pétrologique, *Ph.D. Thesis*, Univ. Clermont-Ferrand II, Clermont-Ferrand, France, 215 pp. (in French).

Bachèlery, P., A. Blum, J. L. Cheminée, L. Chevallier, R. Gaulon, N. Girardin, C. Jaupart, F. Lalanne, J. L. Le Mouel, J. C. Ruegg, and P. Vincent (1982). Eruptions at Le Piton de la Fournaise volcano on 3 February 1981, *Nature* **297,** no. 5865, 395–397 (in French).

Battaglia, J., K. Aki, and V. Ferrazzini (2005). Location of tremor sources and estimation of lava output using tremor source amplitude on the Piton de la Fournaise volcano: 1. Location of tremor sources, *J. Volcanol. Geoth. Res.* **147,** 268–290.

Beauducel, F., D. Lafon, X. Béguin, J. M. Saurel, A. Bosson, D. Mallarino, P. Boissier, C. Brunet, A. Lemarchand, C. Anténor-Habazac, *et al.* (2020). WebObs: The volcano observatories missing link between research and real-time monitoring, *Front. Earth Sci.* **8,** 48, doi: 10.3389/feart.2020.00048.

Beauducel, F., A. Peltier, A. Villié, and W. Suryanto (2020). Mechanical imaging of a volcano plumbing system from GNSS unsupervised modeling, *Geophys. Res. Lett.* **47,** e2020GL089419, doi: 10.1029/2020GL089419.

Biggs, J., and M. E. Pritchard (2017). Global volcano monitoring: What does it mean when volcanoes deform? *Elements* **13,** no. 1, 17–22.

Bonali, F., C. Corazzato, and A. Tibaldi (2011). Identifying rift zones on volcanoes: An example from La Réunion Island, Indian Ocean, *Bull. Volcanol.* **73,** no. 3, 347–366, doi: 10.1007/s00445-010-0416-1.

Boudoire, G., A. Di Muro, M. Liuzzo, V. Ferrazzini, A. Peltier, S. Gurrieri, L. Michon, G. Giudice, P. Kowalski, and P. Boissier (2017). New perspectives on volcano monitoring in a tropical environment: Continuous measurements of soil CO_2 flux at Piton de la Fournaise (La Réunion Island, France), *Geophys. Res. Lett.* **44,** 8244–8253, doi: 10.1002/2017GL074237.

Chevrel, M. O., J. Labroquère, A. J. L. Harris, and S. K. Rowland (2018). PyFLOWGO: An open-source platform for simulation of channelized lava thermo-rheological properties, *Comput. Geosci.* **111,** 167–180.

Chouet, B. A. (1996). Long-period volcano seismicity: Its source and use in eruption forecasting, *Nature* **380,** 309–316, doi: 10.1038/380309a0.

Chouet, B. A., and R. S. Matoza (2013). A multi-decadal view of seismic methods for detecting precursors of magma movement and eruption, *J. Volcanol. Geoth. Res.* **252,** 108–175.

Coppola, D., A. Di Muro, A. Peltier, N. Villeneuve, V. Ferrazzini, M. Favalli, P. Bachèlery, L. Gurioli, A. J. L. Harris, S. Moune, *et al.* (2017). Shallow system rejuvenation and magma discharge trends at Piton de la Fournaise volcano (La Réunion Island), *Earth Planet. Sci. Lett.* **463,** 13–24.

Coppola, D., M. Laiolo, C. Cigolini, F. Massimetti, D. Delle Donne, M. Ripepe, H. Arias, S. Barsotti, C. Bucarey Parra, G. Riky, *et al.* (2020). Thermal remote sensing for global volcano monitoring: Experiences from the MIROVA system, *Front. Earth Sci.* **7,** 362, doi: 10.3389/feart.2019.00362.

Duputel, Z., O. Lengliné, and V. Ferrazzini (2019). Constraining spatiotemporal characteristics of magma migration at Piton de la Fournaise volcano from pre-eruptive seismicity, *Geophys. Res. Lett.* **46,** no. 1, 119–127.

Favalli, M., M. T. Pareschi, A. Neri, and I. Isola (2005). Forecasting lava flow paths by a stochastic approach, *Geophys. Res. Lett.* **32,** L03305, doi: 10.1029/2004GL021718.

Francis, P. W. (1979). Infra-red techniques for volcano monitoring and prediction—A review, *J. Geol. Soc.* **136,** 355–359.

Galle, B., M. Johansson, C. Rivera, Y. Zhang, M. Kihlman, C. Kern, T. Lehmann, U. Platt, S. Arellano, and S. Hidalgo (2010). Network for Observation of Volcanic and Atmospheric Change (NOVAC)—A global network for volcanic gas monitoring: Network layout and instrument description, *J. Geophys. Res.* **115,** D05304, doi: 10.1029/2009JD011823.

Gouhier, M., Y. Guéhenneux, P. Labazuy, P. Cacault, J. Decriem, and S. Rivet (2016). HOTVOLC: A web-based monitoring system for volcanic hot spots, *Geol. Soc. Lond. Spec. Publ.* **426,** 223–241, doi: 10.1144/SP426.31.

Guéhenneux, Y., M. Gouhier, and P. Labazuy (2015). Improved space borne detection of volcanic ash for real-time monitoring using 3-band method, *J. Volcanol. Geoth. Res.* **293,** 25–45.

Gurioli, L., A. Di Muro, I. Vlastélic, S. Moune, N. Villeneuve, P. Bachèlery, M. Valer, S. Thivet, G. Boudoire, A. Peltier, *et al.* (2018). Integrating field, textural and geochemical monitoring to track eruptive triggers and dynamics: The case-study of Piton de la Fournaise 2014 opening eruption, *Solid Earth* **9,** 431–455, doi: 10.5194/se-9-431-2018.

Harris, A., M. O. Chevrel, D. Coppola, M. S. Ramsey, A. Hrysiewicz, S. Thivet, N. Villeneuve, M. Favalli, A. Peltier, P. Kowalski, *et al.* (2019). Validation of an integrated satellite-data-driven response to an effusive crisis: The April–May 2018 eruption of Piton de la Fournaise, *Ann. Geophys.* **62,** 2, VO30, doi: 10.4401/ag-7972.

Harris, A., N. Villeneuve, A. Di Muro, V. Ferrazzini, A. Peltier, D. Coppola, M. Favalli, P. Bachèlery, J. L. Froger, L. Gurioli, *et al.* (2017). Effusive crises at Piton de la Fournaise 2014–2015: A review of a multi-national response model, *J. Appl. Volcanol.* **6,** 11, doi: 10.1186/s13617-017-0062-9.

Harris, A. J. L., J. Dehn, and S. Calvari (2007). Lava effusion rate definition and measurement: A review, *Bull. Volcanol.* **70,** 1–22, doi: 10.1007/s00445-007-0120-y.

Harris, A. J. L., L. P. Flynn, K. Dean, E. Pilger, M. Wooster, C. Okubo, P. Mouginis-Mark, H. Garbeil, S. De la Cruz Reyna, C. Thornber, *et al.* (2000). Real-time monitoring of volcanic hot spots with satellites, *American Geophysical Union Monograph Series*, 116, 139–159.

Harris, A. J. L., E. Pilger, L. P. Flynn, H. Garbeil, P. J. Mouginis-Mark, J. Kauahikaua, and C. Thornber (2001). Automated, high temporal resolution, thermal analysis of Kilauea volcano, Hawaii, using GOES-9 satellite data, *Int. J. Remote Sens.* **22,** no. 6, 945–967.

Hulley, G. C., S. J. Hook, E. Abbott, N. Malakar, T. Islam, and M. Abrams (2015). The ASTER Global Emissivity Dataset (ASTER GED): Mapping Earth's emissivity at 100 meter spatial scale, *Geophys. Res. Lett.* **42,** 7966–7976, doi: 10.1002/2015GL065564.

Journeau, C., N. M. Shapiro, L. Seydoux, J. Soubestre, V. Ferrazzini, and A. Peltier (2020). Detection, classification, and location of seismo-volcanic signals with multi-component seismic data, example from the Piton de la Fournaise volcano (La Réunion, France), *J. Geophys. Res.* **125,** e2019JB019333, doi: 10.1029/2019JB019333.

Lengliné, O., Z. Duputel, and V. Ferrazzini (2016). Uncovering the hidden signature of a magmatic recharge at Piton de la Fournaise volcano using small earthquakes, *Geophys. Res. Lett.* **43,** no. 9, 4255–4262.

Michon, L., F. Saint-Ange, P. Bachèlery, N. Villeneuve, and T. Staudacher (2007). Role of the structural inheritance of the oceanic lithosphere in the magmato-tectonic evolution of Piton de la Fournaise volcano (La Réunion Island), *J. Geophys. Res.* **112,** no. B4, doi: 10.1029/2006JB004598.

Mouginis-Mark, P. J., D. C. Pieri, P. W. Francis, L. Wilson, S. Self, W. I. Rose, and C. A. Wood (1989). Remote sensing of volcanoes and volcanic terrains, *EOS* **70,** no. 52, 1567–1575.

Mouginis-Mark, P. J., H. Snell, and R. Ellisor (2000). GOES satellite and field observations of the 1998 eruption of Volcan Cerro Azul, Galápagos, *Bull. Volcanol.* **62,** 188–198.

Moune, S., F. Faure, P. J. Gauthier, and K. W. W. Sims (2007). Pele's hairs and tears: Natural probe of volcanic plume, *J. Volcanol. Geoth. Res.* **164,** 244–253.

Nikkhoo, N., T. R. Walter, P. R. Lundgren, and P. Prats-Iraola (2017). Compound dislocation models (CDMs) for volcano deformation analyses, *Geophys. J. Int.* **208,** 877–894, doi: 10.1093/gji/ggw427.

Pallister, J., P. Papale, J. Eichelberger, C. Newhall, C. Mandeville, S. Nakada, W. Marzocchi, S. Loughlin, G. Jolly, J. Ewert, *et al.* (2019). Volcano observatory best practices (VOBP) workshops —A summary of findings and best-practice recommendations, *J. Appl. Volcanol.* **8,** 2, doi: 10.1186/s13617-019-0082-8.

Peltier, A., P. Bachèlery, and T. Staudacher (2009). Magma transfer and storage at Piton de la Fournaise (La Réunion Island) between 1972 and 2007: A review of geophysical and geochemical data, *J. Volcanol. Geoth. Res.* **184,** nos. 1/2, 93–108.

Peltier, A., F. Beauducel, N. Villeneuve, V. Ferrazzini, A. Di Muro, A. Aiuppa, A. Derrien, K. Jourde, and B. Taisne (2016). Deep fluid transfer evidenced by surface deformation during the 2014–2015 unrest at Piton de la Fournaise volcano, *J. Volcanol. Geoth. Res.* **321,** 140–148, doi: 10.1016/j.jvolgeores.2016.04.031.

Peltier, A., J. L. Froger, N. Villeneuve, and T. Catry (2017). Assessing the reliability and consistency of InSAR and GNSS data for retrieving 3D displacement rapid changes, the example of the 2015 Piton de la Fournaise eruptions, *J. Volcanol. Geoth. Res.* **344,** 106–120, doi: 10.1016/j.jvolgeores.2017.03.027.

Peltier, A., N. Villeneuve, V. Ferrazzini, S. Testud, T. Hassen Ali, P. Boissier, and P. Catherine (2018). Changes in the long-term geophysical eruptive precursors at Piton de la Fournaise: Implications for the response management, *Front. Earth Sci.* **6,** 104, doi: 10.3389/feart.2018.00104.

Philipson, G., R. Sobradelo, and J. Gottsmann (2013). Global volcanic unrest in the 21st century: An analysis of the first decade, *J. Volcanol. Geoth. Res.* **264,** 183–196.

Pinel, V., M. P. Poland,, and A. Hooper (2014). Volcanology: Lessons learned from synthetic aperture radar imagery, *J. Volcanol. Geoth. Res.* **289,** no. 1, 81–113.

Poland, M. P., T. Lopez, R. Wright, and M. J. Pavolonis (2020). Forecasting, detecting, and tracking volcanic eruptions from space, *Remote Sens. Earth Syst. Sci.* **3,** 55–94, doi: 10.1007/s41976-020-00034-x.

Ramsey, M. (2016). Enhanced volcanic hot-spot detection using MODIS IR data: Results from the MIROVA system, in *Detecting, Modelling and Responding to Effusive Eruptions*, A. J. L. Harris, T. De Groeve, F. Garel, and S. A. Carn (Editors), Vol. 426, Geological Society, London, Special Publications, 181–205, doi: 10.1144/SP426.5.

Ramsey, M. S., and A. J. L. Harris (2013). Volcanology 2020: How will thermal remote sensing of volcanic surface activity evolve over the next decade? *J. Volcanol. Geoth. Res.* **249,** 217–233.

Richter, N, and J. L. Froger (2020). The role of Interferometric Synthetic Aperture Radar in detecting, mapping, monitoring, and modelling the volcanic activity of Piton de la Fournaise, La Réunion: A review, *Remote Sens.* **12,** 1019.

Roach, A. L., J. P. Benoit, K. G. Dean, and S. R. McNutt (2001). The combined used of satellite and seismic monitoring during the 1996 eruption of Pavlof volcano, Alaska, *Bull. Volcanol.* **62,** 385–399, doi: 10.1007/s004450000114.

Rothery, D. A. (1992). Monitoring and warning of volcanic eruptions by remote sensing, in *Geohazards: Natural and Man-Made*,G. J. H. McCall, D. J. C. Laming, and S. C. Scott (Editors), Chapman & Hall, London, 25–32.

Roult, G., A. Peltier, B. Taisne, T. Staudacher, V. Ferrazzini, A. Di Muro, and the OVPF group (2012). A new comprehensive classification of the Piton de la Fournaise eruptions spanning the 1986–2011 period. Search and analysis of eruption precursors from a broad-band seismological station, *J. Volcanol. Geoth. Res.* **241/242,** 78–104.

Sundermeyer, C., A. Di Muro, B. Gordeychik, and G. Wörner (2020). Timescales of magmatic processes during the eruptive cycle 2014–2015 at Piton de la Fournaise, La Réunion, obtained from Mg–Fe diffusion modelling in olivine, *Contrib. Mineral. Pet.* **175,** no. 1, 1.

Thivet, S, L. Gurioli, A. Di Muro, J. Eychenne, P. Besson, and J. M. Nedelec (2020). Variability of ash deposits at Piton de la Fournaise (La Reunion Island): Insights into fragmentation processes at basaltic shield volcanoes, *Bull. Volcanol.*, **82,** doi: 10.1007/s00445-020-01398-0.

Tilling, R. I. (1987). Introduction to special section on how volcanoes work: Part 1, *J. Geophys. Res.* **92,** no. B13, 13,685–13,686.

Tulet, P., A. Di Muro, A. Colomb, C. Denjean, V. Duflot, S. Arellano, B. Foucart, J. Brioude, K. Sellegri, A. Peltier, *et al.* (2017). First results of the Piton de la Fournaise STRAP 2015 experiment: Multidisciplinary tracking of a volcanic gas and aerosol plume, *Atmos. Chem. Phys.* **17,** 5355–5378, doi: 10.5194/acp-17-5355-2017.

Villeneuve, N., and P. Bachèlery (2006). Revue de la Typologie des Eruptions au Piton de la Fournase, Processus et Risqué Volcaniques Associés, Cybergeo, available at http://cybergeo.revues.org/index2536.html (in French).

Manuscript received 8 June 2020
Published online 11 November 2020